Supplementary Information

Interplay between myosin IIA-mediated contractility and actin network integrity orchestrates podosome composition and oscillations

K. van den Dries, M. Meddens, S. de Keijzer, S. Shekhar, V. Subramaniam, C.G. Figdor and A. Cambi

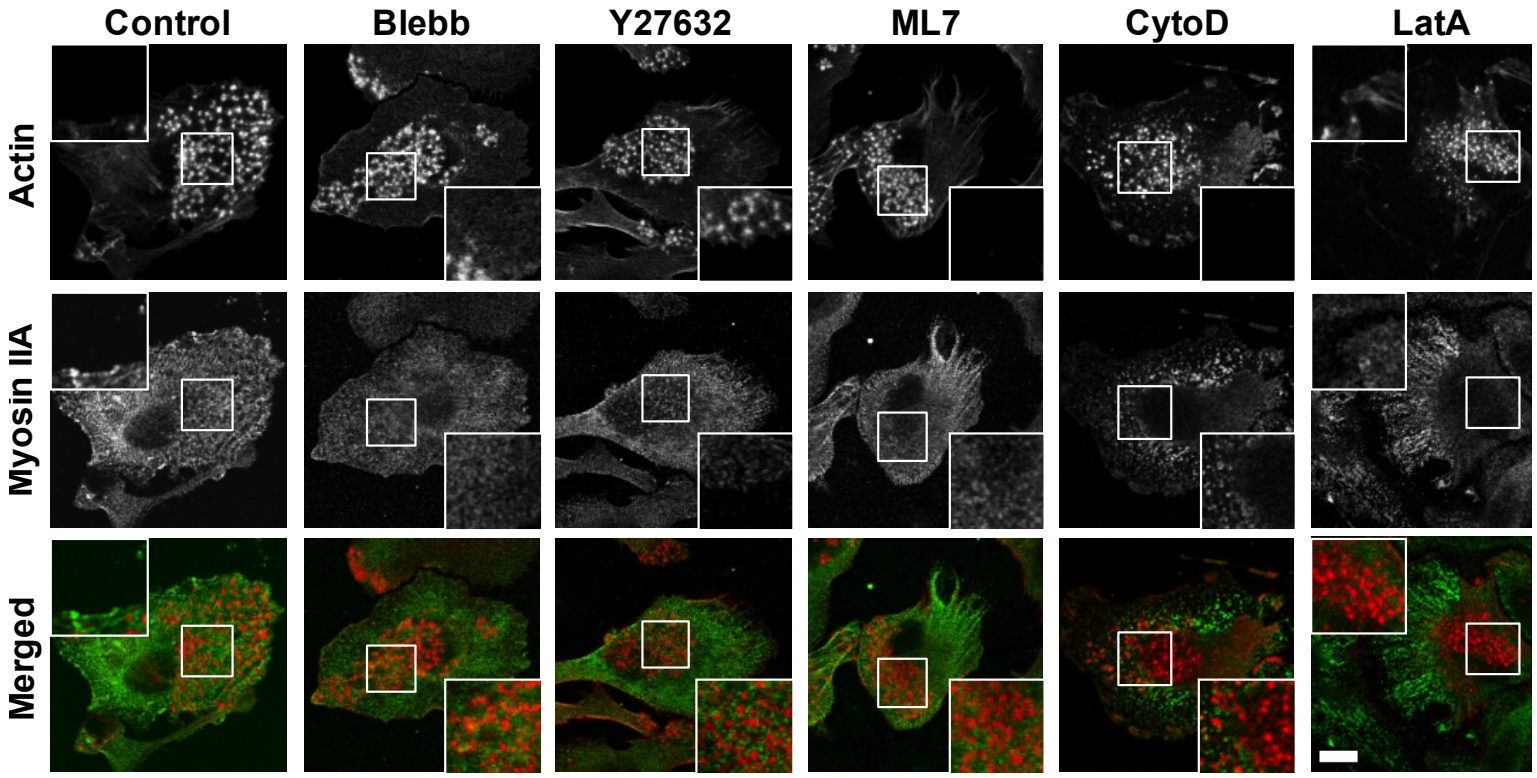

Supplementary Figure S1. Immunolocalization of myosin IIA after stimulation with actomyosin disrupting drugs Cells were seeded on glass coverslips and left to adhere for 3 hrs. Cells were subsequently left untreated or stimulated with 20µM blebb, 20µM Y27632, 20µM ML7 for 30 min or 2.5µg/ml CytoD, 2µg/ml LatA for 2min. Next, cells were fixed, permeabilized and stained with Texas Red-conjugated phalloidin and an anti-myosin IIA monoclonal antibody. Blebb induces the complete dislocation of myosin IIA from the actin filaments in DCs, while treatment with Y27632 and ML7 leaves the actomyosin network unaffected. Stimulation with CytoD and LatA resulted in a complete disruption of the actin network and therefore also a relocation of myosin IIA within DCs. Scale bar, 10 µm.

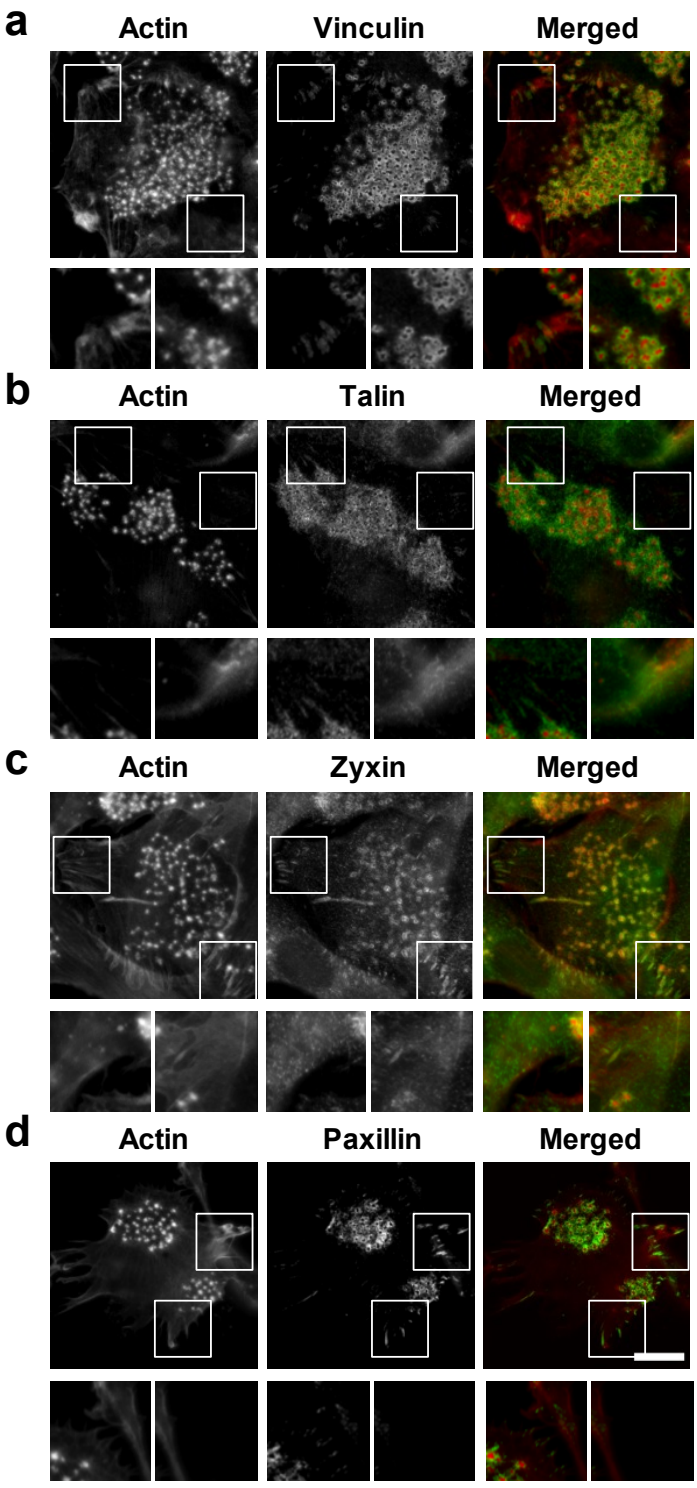

Supplementary Figure S2. DCs spontaneously form numerous bona fide FAs Cells were seeded on glass coverslips and left to adhere for 3 hrs. Cells were subsequently fixed and stained with Texas Red-conjugated phalloidin and specific antibodies to visualize actin and the FA markers a) vinculin, b) talin, c) zyxin and d) paxillin, respectively. For every marker, two regions containing multiple FAs are magnified to show the presence of all four markers. Scale bar, 10 µm.

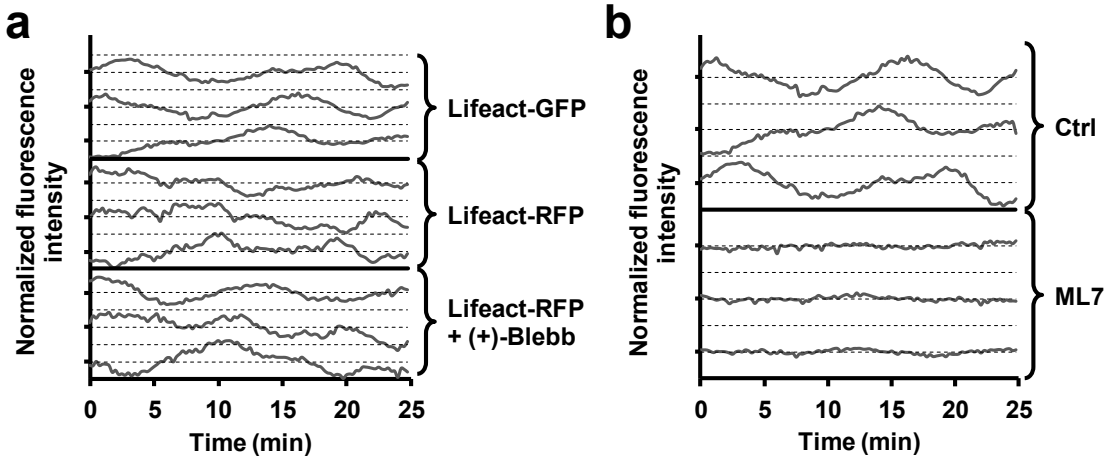

Supplementary Figure S3. Podosome oscillatory behaviour in DCs a) Cells were transfected with Lifeact-GFP or –RFP, seeded on glass coverslips and intensity fluctuations were measured for individual podosomes in untreated control cells. Also shown are the intensity fluctuations of lifeact-RFP in the presence of inactive (+)-blebbistatin. b) cells were transfected with Lifeact-GFP, seeded on glass coverslips and intensity fluctuations were measured for individual podosomes in untreated color cells (Ctrl) and cells treated with 20 µM ML7 (ML7).

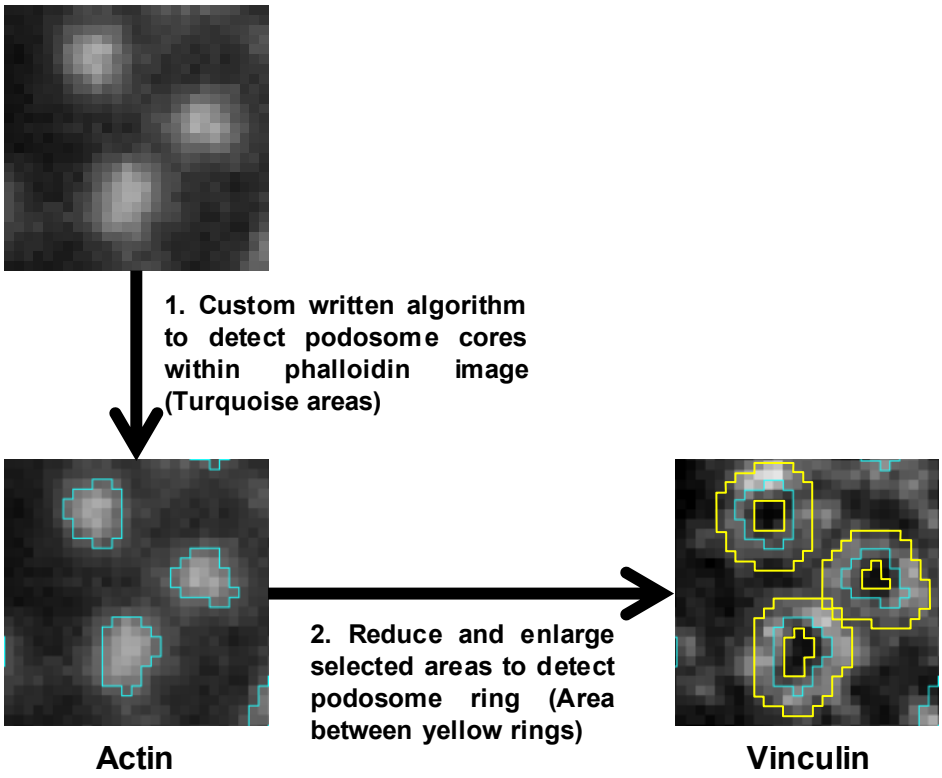

Supplementary Figure S4. Overview of image analysis Cells were seeded onto glass coverslips, fixed and subsequently stained with Texas Red-conjugated phalloidin and a monoclonal vinculin antibody to visualize actin and vinculin, respectively. A custom written algorithm which exploits local and global intensity thresholding was used to detect the podosome cores within the phalloidin image (Meddens et al, *Microsc Microanal*, *In Press* DOI:10.1017/S1431927612014018). This area (here indicated in turquoise) was used for the analysis in Figure 2f. Thereafter, the original area was eroded by 1 pixel and dilated by 2 pixels (indicated by two yellow lines). The area in between the two yellow lines delineates the ring area and was used for the intensity analysis in Figure 3e and 5e.

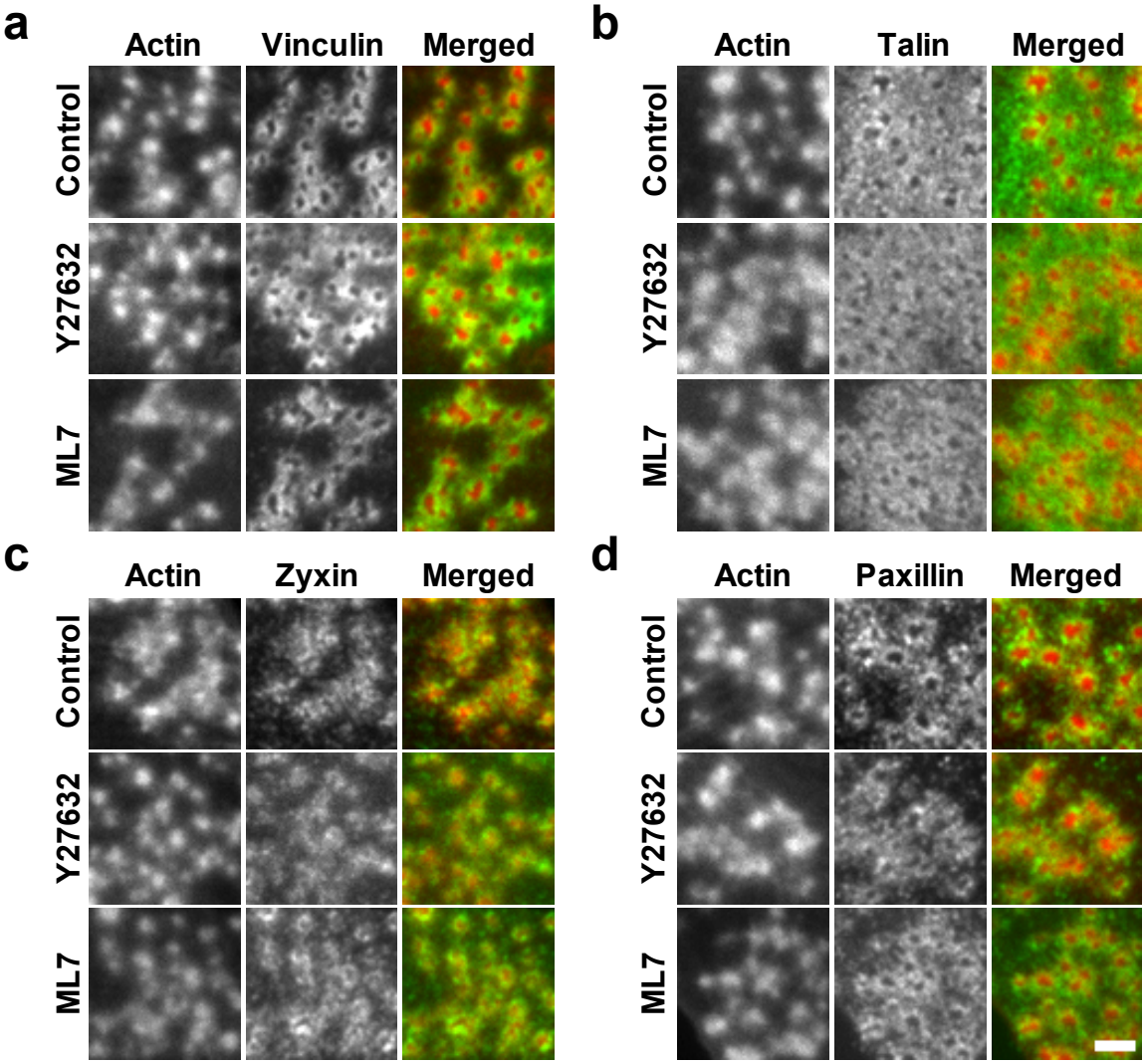

Supplementary Figure S5. Immunolocalization of adaptor proteins after stimulation with Y27632 or ML7 Immunolocalization of actin (red) with either (in green) a) vinculin, b) talin, c) zyxin and d) paxillin in untreated control cells (upper row) and cells treated for 30 min. with 20µM of the ROCK inhibitor Y27632 (middle row) or 20µM of the MLCK inhibitor ML7 (lower row). Actin was stained by Texas-Red phalloidin, whereas adaptor proteins were labelled by specific mAbs and subsequently secondary antibodies conjugated to Alexa488. Merged images are shown on the right. Images are representative of multiple cells from at least three similar experiments. Scale bar, 2 µm.

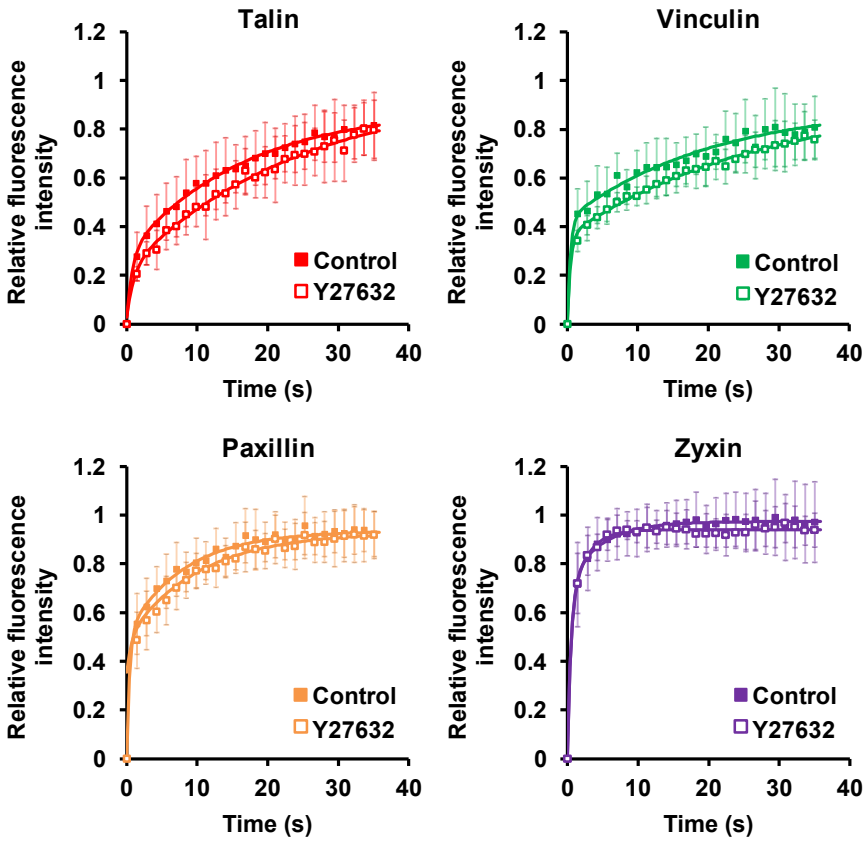

Supplementary Figure S6. Diffusion of adaptor proteins within podosomes is myosin IIA-independent Cells were transfected with GFP-tagged vinculin, talin, paxillin and zyxin and individual podosomes were subjected to FRAP. Shown is the average fluorescent recovery for the four adaptor proteins in the absence (closed boxes) or presence (open boxes) of the ROCK inhibitor Y27632 for at least 10 podosomes in 5 different cells. The error bars indicate the standard deviation. The average FRAP curves were fitted with a two component association model (see Material and Methods), which are shown as solid lines through the data points.

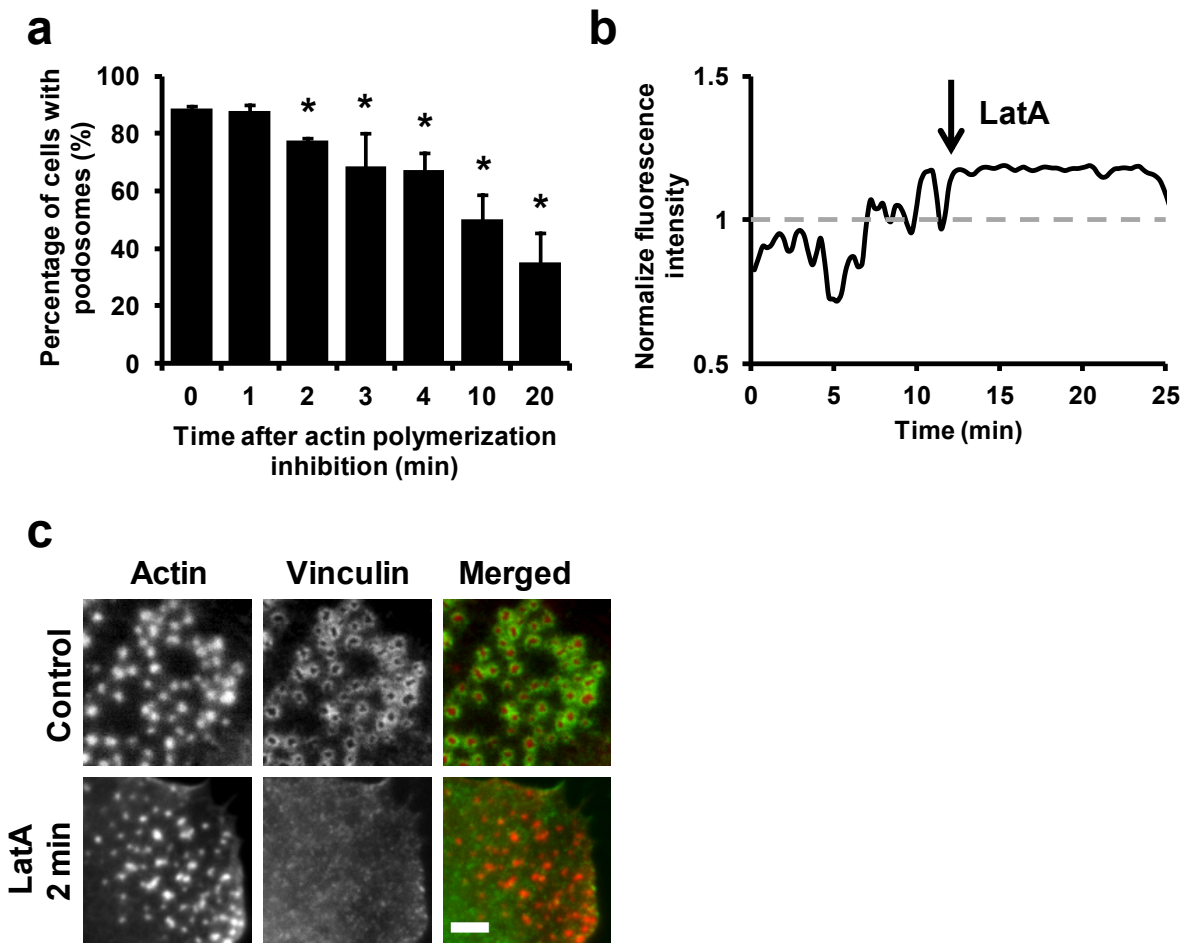

Supplementary Figure S7. Inhibition of actin polymerization leaves the core intact but disrupts podosome ring integrity. a) Quantification of cells bearing podosomes after cytoD stimulation. b) Actin levels, visualized by Lifeact-GFP, over time for a representative podosome core. The arrow indicates the addition of latrunculin A (latA). Data are normalized to average intensity. c) Immunolocalization of actin (red) and vinculin (green) in untreated cells (upper row) or cells treated with latA for 2 min. (lower row). Scale bar, 3 µm.

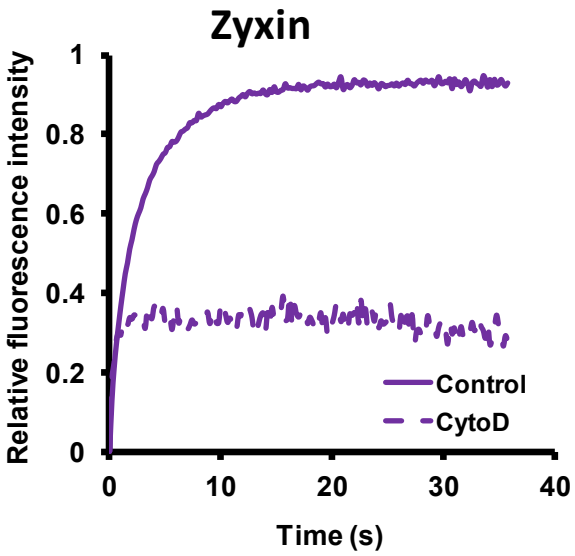

Supplementary Figure S8. Slow fraction of zyxin is completely static after inhibition of actin polymerization DCs were transfected with zyxin-GFP and individual podosomes were subjected to FRAP. Shown are the average fluorescence recovery curves for at least 10 podosomes in 5 different cells. The initial fast recovery is due to the unbound cytosolic fraction and appears insensitive to cytoD treatment. In contrast, cytoD treatment appears to abolish the turnover of the bound zyxin as shown by the increase in immobile population. We could not determine the diffusion of the other adaptor proteins after cytoD stimulation since they either left the podosome ring too rapidly (as in the case of vinculin and paxillin) or their levels were too low and steadily decreasing over time (talin), which made FRAP analysis unfeasible.

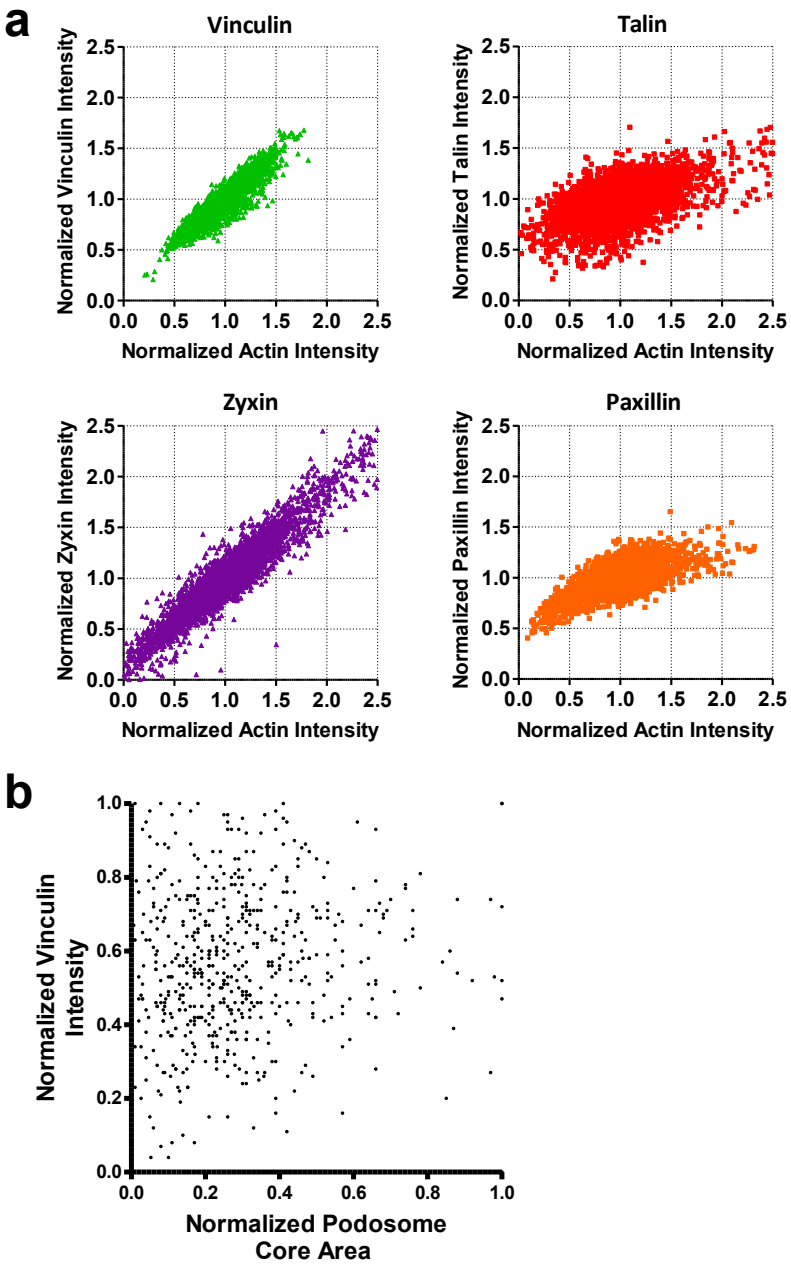

Supplementary Figure S9. Adaptor proteins levels differentially correlate with actin core levels a) Total datasets for the correlation between vinculin, talin, zyxin and paxillin levels in the podosome ring and the actin levels in the core. Data were normalized to the average intensity. b) Cells were cotransfected with Lifeact-RFP and vinculin-GFP, seeded on coverslips and fixed after 16 hours. Images of double positive cells were collected and the average vinculin intensity was correlated with the podosome core area. Subsequently, podosome area was calculated, binned and correlated with the vinculin ring intensity for at least 500 podosomes in 5 different cells. It has to be noted that this analysis was performed on the same podosomes as shown in Figure 6e. Both datasets are linearly normalized between the minimum and maximum value.

Supplementary Table S1. Fitting parameters of the correlation between the levels of the four adaptor proteins and actin within podosomes

	Linear fit			
	Vinculin	**Talin**	**Zyxin**	**Paxillin**
Slope	0.818	0.2928	0.8512	0.3239
Range	0.8052 - 0.8307	0.2797 - 0.3058	0.8426 - 0.8597	0.3128 - 0.3351
R-squared	0.8338	0.3068	0.8971	0.4239

	One phase decay fit			
	Vinculin	**Talin**	**Zyxin**	**Paxillin**
Plateau	≈ 12.30	1.735	≈ 73.00	1.263
Range	(Very wide)	1.482 - 1.988	(Very wide)	1.228 - 1.297
R-squared	0.8339	0.3115	0.8971	0.46